Control of the size of the coherence area in entangled twin beams

M. W. Holtfrerich and A. M. Marino*

Homer L. Dodge Department of Physics and Astronomy, University of Oklahoma, 440 West Brooks Street, Norman, Oklahoma 73019, USA

(Received 9 February 2016; published 13 June 2016)

We study the effect of a change in size and spatial profile of the pump beam in an atomic-based four-wave mixing process on the size of the coherence area of the generated entangled twin beams. We perform experiments and develop a theoretical model to obtain a measure of the linear extent or "radius" of the coherence area from noise measurements of the twin beams as a function of transmission through a variable size slit. Our results show that an increase in the size of the pump reduces the size of the coherence area. More interestingly, we find that the use of a flat-top pump beam of the same size as a Gaussian pump beam leads to a reduction by a factor of more than 2 in the linear extent of the coherence area. This in turn leads to an increase by a factor of more than 4 in the number of spatial modes that make up the twin beams and a resolution enhancement of the entangled images that can be generated with the four-wave mixing process.

DOI: 10.1103/PhysRevA.93.063821

The study of the spatial quantum correlations in entangled beams of light has become an active research area due to the role that these quantum correlations play in the field of quantum imaging [1,2], which promises to improve optical resolution [3] and image detection [4] and to enhance quantum information through quantum holographic teleportation [5], quantum holograms [6], and parallel quantum information encoding [7]. Spatial quantum correlations are a result of having entangled beams of light composed of multiple spatial modes. Each of these modes can be viewed as an independent quantum channel that can be used to transmit information or to probe different spatial regions of a two-dimensional sample for enhanced imaging [8]. The study of these spatial quantum correlations has also extended to the field of matter waves, where the spatial properties of matter four-wave mixing in ultracold atoms have been studied both theoretically and experimentally [9–11].

The presence of spatial quantum correlations in entangled beams of light is an indication that different corresponding subregions of the beams are independently entangled with each other. The smallest size of these independently correlated subregions is known as the coherence area. The coherence area limits the resolution of the entangled images that can be generated and is ultimately linked to the number of spatial modes that make up the entangled beams [12]. Thus the ability to control the size of the coherence area provides a method to control the number of spatial modes and the information density of a quantum channel.

The possibility of modifying the size of the coherence area was first realized theoretically [13] when studying the effects of focusing the pump beam for the generation of entangled photon pairs with parametric down conversion (PDC). Since then, there have been a number of experiments that have studied the dependence of the spatial quantum correlations on the spatial profile of the pump using PDC [14–18]. The work done to date, however, has been mainly limited to the discrete domain and the changes on the spatial quantum correlations have been limited due to the phase-matching condition in PDC.

In this paper we study the effect of the size and shape of the pump beam in a four-wave mixing process (FWM) on the size of the coherence area. This process leads to the generation of bright entangled beams of light, or twin beams, which are the foundation for continuous-variable (CV) quantum information. The use of CVs offers advantages over the discrete regime of entangled photon pairs, such as the possibility of deterministically generating entangled states that can be measured with high efficiency and that can be efficiently mapped onto atomic ensembles. We perform experiments and develop a model that allows us to extract the linear extent or "radius" of the coherence area based on noise measurements of one of the twin beams after propagation through a variable size slit. Finally, we study the effect of the size of the coherence area on the resolution of the entangled images that can be generated with the FWM process.

I. EXPERIMENTAL SETUP

We use FWM in a double-Λ configuration in atomic rubidium vapor to generate bright entangled twin beams, which we call probe and conjugate [19]. We have previously shown that this process generates entangled twin beams that are highly multi-spatial-mode [12], which makes it possible to generate entangled images [20]. This makes this system ideal for controlling the size of the coherence area, which translates into the ability to control the number of spatial modes that make up the twin beams.

We implement the FWM process by intersecting a strong pump beam and a weak probe beam inside a ^{85}Rb cell at a small angle, as shown in Fig. 1. In this configuration, the strong pump beam acts as the two pumps that are required for the FWM process. The pump and the probe, with angular frequencies ω_0 and $\omega_p < \omega_0$, respectively, are tuned around 1 GHz to the blue of the $D1$ line at 795 nm. The pump and probe are resonant with a two-photon Raman transition between the two electronic ground states $F = 2$ and $F = 3$, which are separated by 3 GHz. As a result of the FWM process, the probe beam is amplified and a new beam, the conjugate, is generated. The coupling between the light fields and the atomic levels follows a double-Λ configuration [21–24] that converts two photons

*marino@ou.edu

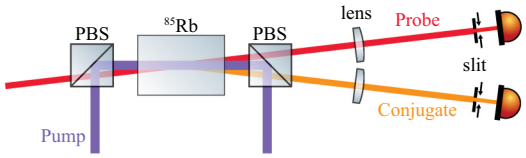

FIG. 1. Experimental setup. A FWM process is used to generate quantum-correlated bright twin beams. After the Rb cell, lenses are used to obtain the Fourier transform of the center of the cell to study the spatial quantum correlations in the far field through noise measurements after transmission through variable size slits. PBS = polarizing beam splitter.

from the pump into one probe photon and one conjugate photon at frequency $\omega_c = 2\omega_0 - \omega_p$.

The spatial quantum correlations between the generated probe and conjugate are a result of the conservation of momentum, or phase-matching condition, in the FWM process. For a pump beam that can be approximated as a plane wave (single k-vector) the phase-matching condition dictates that a single k-vector of the probe is anticorrelated with a single k-vector of the conjugate. This means that in the far field the spatial correlations between the probe and the conjugate are point-to-point correlations. For a finite-size pump beam, such as one with a Gaussian transverse profile, there will be a spread of k-vectors for the pump that in turn will lead to a spread of the spatial quantum correlations between the probe and the conjugate. This will make a point in the probe be correlated with a region in the conjugate, which corresponds to the coherence area [25]. The number of coherence areas that fit into the angular bandwidth of the process (given by the angular range due to the phase-matching condition over which the FWM can occur) gives a measure of the number of spatial modes that make up the twin beams [12]. As a result, controlling the size of the coherence area also controls the number of spatial modes. In particular, if a single coherence area makes up the entire beam then the twin beams are single mode; otherwise they are spatially multimode.

Formally, for an intrinsically multimode state of light there does not exist a basis that can describe the system as having all the photons reside in a single mode with a wave function of the form [26]

$$|\psi\rangle \neq |\phi\rangle_0 \otimes |0\rangle_1 \otimes \cdots \otimes |0\rangle_i \cdots , \tag{1}$$

where the subscript indicates the optical mode coupled to the medium. In order to study the multi-spatial-mode nature of a beam of light it is necessary to perform a noise analysis of different spatial regions of the beams. While the coherence area is a concept that relates the spatial correlations between the twin beams, it also has an impact on the noise properties of the individual beams and sets a length scale for the noise properties of each beam.

After the Rb cell, a 1 m focal length lens is used to obtain the Fourier transform of the center of the cell in order to study the spatial properties of the twin beams in the far field, as shown in Fig. 1. We analyze the spatial distribution of the quantum correlations by placing a slit of variable width at the Fourier plane of either the probe or the conjugate beam. We then use a photodiode to detect the probe or the conjugate beam as we change the size of the slit. Finally, we use a spectrum analyzer to obtain the noise properties of the beam as a function of the transmitted power through the variable slit. The dependence of the noise on the transmission provides a direct confirmation of the multi-spatial-mode nature of the twin beams. In the case of a single spatial mode, the noise changes linearly as a function of transmission, independently of the attenuation mechanism. However, for the case of a multi-spatial-mode beam a deviation from the linear dependence is obtained [12,26]. Similar experiments related to determining the number of modes by cutting the beams have been previously performed both for the spatial domain [12] and the temporal domain [27].

TABLE I. Experimental parameters for the FWM process for the different pump beams.

	Gaussian			Flat top
Pump diameter (mm)	1.5	2.3	3.2	3
Pump power (W)	0.24	0.47	0.86	2.25
FWM gain	3.5	3.5	3.5	3.5
Squeezing (dB)	4.0	4.5	4.0	3.0

We perform a series of measurements with different sizes and profiles for the pump beam to study the effect of a change of the pump on the coherence area. In particular, we consider a pump beam with a Gaussian profile and a $1/e^2$ diameters of 1.5 mm, 2.3 mm, and 3.2 mm as well as a pump with a flat-top profile and a diameter of 3.0 mm. The flat top was generated by using a refractive optical beam shaper that allows us to transfer over 90% of the power from the Gaussian profile to the flat-top profile. After the beam shaper a 4f optical system is used to image the flat top to the center of the cell, such that the pump field at the center of the cell has a flat-top profile with a flat uniform wave front. We verified that the flat-top profile of the pump remains nearly unchanged throughout the length of the cell. The total power for each of the different pump beams used was selected such that a similar gain and intensity-difference squeezing was obtained from the FWM process. This makes it possible to compare each of the configurations under similar conditions, as effects such as gain narrowing [28] can lead to a modification of the size of the coherence area. Table I shows the specific values for the pump power, FWM gain, and intensity-difference squeezing for each of the pump beams. For all the measurements, the probe beam had a $1/e^2$ diameter of 0.37 mm at the center of the cell and an input power of $\sim$40 μW. The temperature of the cell was 117 °C, which corresponds to a number density of $\sim 2 \times 10^{13}$ cm^{-3}.

II. EXPERIMENTAL RESULTS

To characterize the noise properties of the probe or conjugate beam after transmission through the slit we use the Mandel Q parameter defined as

$$Q = \frac{\langle(\triangle \hat{N})^2\rangle}{\langle \hat{N} \rangle} - 1, \tag{2}$$

where $\hat{N}$ is the number photon operator. The Q parameter represents the intensity noise normalized to the noise of a coherent state of the same intensity (i.e., the standard quantum

limit or SQL) minus one, such that $Q = 0$ corresponds to the SQL. When a beam of light is uniformly attenuated with a beam splitter or a neutral density filter, Q varies linearly as a function of the transmitted intensity from its initial value for unit transmission to 0 for no transmission. As shown in Ref. [29], for a single-spatial-mode beam the Q parameter varies linearly independently of how the beam is attenuated. This means that if a single-spatial-mode beam is partially blocked its Q parameter varies as if the beam had been uniformly attenuated, that is, linearly as a function of transmission. On the other hand, for a multi-spatial-mode field the change of the Q parameter as a function of attenuation will be different depending on the method that is used to attenuate it. In particular, if a variable slit is used to attenuate the beam, the Q parameter will no longer change linearly with the transmitted power.

While we performed measurements on both the probe and the conjugate, we concentrate on the conjugate since it provides a cleaner system to perform the measurements due to the cross-Kerr effect with the pump. Even though this effect is present for both the probe and the conjugate, it is only significant for the probe given that the conjugate is around 4 GHz away from resonance. The cross-Kerr effect introduces additional complications when performing measurements on the probe beam that can be ignored for the conjugate beam.

Figure 2 shows the normalized Q parameter, Q_N, as a function of transmission through the variable slit for the different pump beams when measurements are performed on the conjugate beam. For these measurements the variable slit was always centered on the conjugate beam and its size was changed from 2 mm, which corresponds to twice the diameter of the conjugate beam, to completely closed. After the slit an optical system was used to image the slit onto to the detector. For each of the measurements the intensity noise, $\langle(\triangle\hat{N})^2\rangle$, of the transmitted conjugate was measured with an RF spectrum analyzer at a frequency of 500 kHz, RBW of 30 kHz, and VBW of 100 Hz. The Q parameter was then calculated by measuring the corresponding SQL and using it to normalize the intensity noise according to Eq. (2). Finally we normalize the calculated Q parameter to its maximum value, Q^0, which occurs when the slit is completely open such that it does not introduce losses.

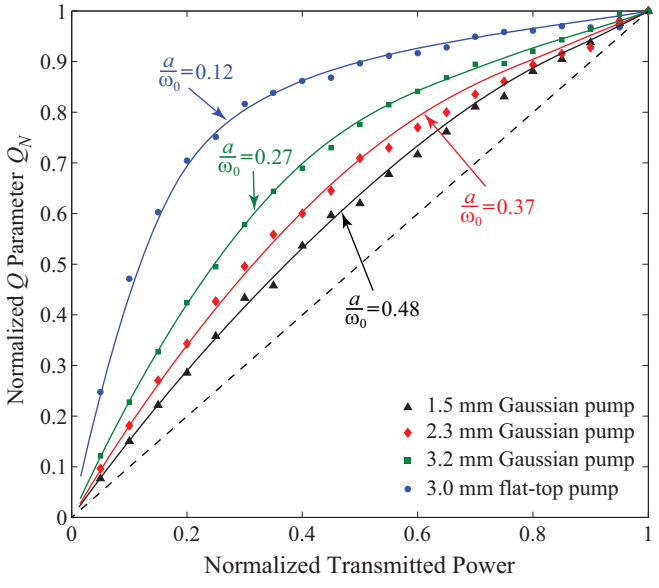

FIG. 2. Experimental results and fit to theoretical model. Normalized Q parameter, Q_N, as a function of transmission through the variable size slit for the 1.5 mm Gaussian pump (black triangles, ▲), 2.3 mm Gaussian pump (red diamonds, ♦), 3.2 mm Gaussian pump (green squares, ■), and 3.0 mm flat-top pump (blue circles, ●). The solid lines show the fits obtained with the theoretical model for each of the different pump beams. The ratio of the linear extent or "radius" of the coherence area, a, to the radius of the conjugate beam, ω_0, obtained from the model is given for each pump configuration. The only free parameter in the model is the linear extent a of the coherence area. The dashed line corresponds to the behavior that would be obtained in the case of a single spatial mode beam.

As can be seen, all the measurements deviate from the straight line that would be obtained if the conjugate were a single mode (dashed line in Fig. 2). In addition, as the pump beam becomes larger, the behavior of Q deviates more and more from the single-mode behavior. More importantly, for the flat-top pump we obtain an even more significant change than for a Gaussian beam of a similar size. While these measurements do not directly provide an estimate of the size of the coherence area, they confirm that for all the different pump beams used the generated twin beams are spatially multimode and that a change of the pump beam has an impact on the spatial structure of the generated conjugate and thus on the coherence area.

We performed similar measurements on the probe beam. While the results we found for the probe were consistent with the ones for the conjugate, care had to be taken to select the correct plane to perform the measurements. Different size pumps led to a different effective focusing due to the cross-Kerr effect between the probe and the pump, which in turn affected the optical system that was used to obtain the Fourier transform. As a result, the position of the Fourier transform plane changed as the size of the pump beam changed. If this change of plane is not properly taken into account then the measurements performed will not provide a correct estimation of the coherence area. The concept of a "localized" coherence area only makes sense in the far field, such that if we are at a different plane the spatial quantum correlations will be more spread out.

We verified the location of the Fourier plane by using an input probe beam with a given pattern, placing its Fourier transform at the center of the cell with an optical system, and then finding the location of the best image after performing the Fourier transform with the 1 m lens after the cell. We also verified that the plane where we obtain the best imaging coincides with the plane where the noise measurements with the variable slit resulted in the smallest size for the coherence area. The location of the correct plane to perform the measurements for the probe shifts closer to the expected location as the pump beam diameter is increased and thus the lensing effect due to the cross-Kerr effect is reduced. For the flat top the location was found to corresponds to the expected plane. We verified that for the conjugate beam, which is far away from atomic resonance, the cross-Kerr effect does not play a significant role and the image as well as the smallest size of the coherence area occur at the expected location independent of the pump beam that is used.

III. THEORETICAL MODEL

In order to obtain a measure of the size of the coherence area from the measurements of the noise as a function of transmission through the variable slit we need to understand the functional form of the Q parameter. To this end we developed a model based on the concept of a localized coherence area. We first expand the field operators in terms of a complete set of transverse spatial modes $A_i(x,y)$ [30]:

$$\hat{a}(x,y) = \sum_i A_i(x,y)\hat{a}_i, \tag{3}$$

where $\hat{a}_i$ is the field operator for mode i. After going through the slit each mode will experience a different loss, such that mode i transforms according to

$$\hat{a}_i \rightarrow \sqrt{\eta_i}\hat{a}_i + \sqrt{1-\eta_i}\hat{a}_{v,i}, \tag{4}$$

where η_i is the transmission of mode i through the aperture and $\hat{a}_{v,i}$ is the corresponding vacuum mode that couples in as a result of losses. With this expansion, the Mandel Q parameter takes the form

$$Q = \frac{\sum_i \eta_i^2[\langle(\Delta\hat{n}_{a,i})^2\rangle - \langle\hat{n}_{a,i}\rangle]}{\sum_i \eta_i\langle\hat{n}_{a,i}\rangle} = \frac{\sum_i \eta_i^2\langle\hat{n}_{a,i}\rangle Q_i^0}{\sum_i \eta_i\langle\hat{n}_{a,i}\rangle}, \tag{5}$$

where Q_i^0 is the Mandel Q parameter for mode i before the slit.

Next, we assume that all the spatial modes have the same normalized noise properties, that is, the same initial Mandel Q parameter: $Q_i^0 \equiv Q^0$. From Eq. (5) it is clear that Q^0 corresponds to the noise in the absence of losses, that is, when $\eta_i = 1$ for all modes. This assumption is valid for our system given the small portion of the angular bandwidth that is covered by the generated bright conjugate beam. Given the size of the probe beam inside the cell, the angular spread of the conjugate is of the order of 2 mrad, while the angular bandwidth of the process is in excess of 10 mrad [12]. With this assumption we find that the normalized Q parameter, Q_N, given by the ratio of the Q parameter after the slit to its maximum value Q^0, takes the form

$$Q_N = \frac{Q}{Q^0} = \frac{\sum_i \eta_i^2\langle\hat{n}_{a,i}\rangle}{\sum_i \eta_i\langle\hat{n}_{a,i}\rangle}. \tag{6}$$

As can be seen from this equation, the functional form of Q_N depends only on the shape of the aperture and how it attenuates the different modes as its size is reduced.

In order to model the concept of a coherence area we need to use a set of spatial modes that are spatially localized and that form a complete orthonormal basis. This can be done by using a basis set that consists of two-dimensional *rect* functions, analogous to the pixels in an image. The use of these modes allows us to develop a model that is independent of the pump configuration of the FWM and to extract a measure of the coherence area based only on the intensity noise measurements. This results in a direct comparison between the different pump beams used as it does not require any assumptions about other competing effects, such as the cross-Kerr effect, that can directly affect the effective size of the coherence area. In particular, we consider a set of square "pixels" of size $2a \times 2a$ as the basis, as shown in Fig. 3(a), where a corresponds to the linear extent or "radius" of the coherence area. Given that the coherence area sets the minimum transverse spatial dimension of any structure on the twin beams, there is no need to consider a basis of a smaller size. In this model we assume each square to be an independent single spatial mode, such that its noise scales linearly with losses, consistent with the concept of the coherence area.

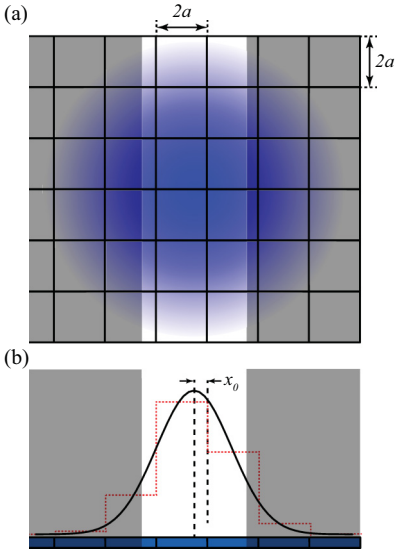

FIG. 3. Theoretical model used for extracting size of coherence area. (a) A discrete basis in the form of square "pixels" of size $2a \times 2a$ is used to model the concept of a localized coherence area. In the model a corresponds to the linear extent or "radius" of the coherence area. (b) Projection along the horizontal direction. The model integrates over the vertical direction as the size of the slit remains constant in that direction. x_0 corresponds to the distance between the center of the projection of the beam and the edge of the closest pixel. The red dotted line shows the discretization of the spatial profile of the beam, shown as a Gaussian, onto the effective one-dimensional pixel basis. The shaded areas represent the region blocked by the variable size slit.

For the problem at hand we can reduce the above analysis to a one-dimensional problem as the size of the slit is only changed in one direction. Effectively we integrate over the spatial profile of the beam along the direction over which the size of the slit remains constant, as illustrated in Fig. 3(b). Given the discrete nature of the basis, the alignment of the center of the spatial profile of the beam with respect to the "pixel" basis plays a role in the evaluation of Eq. (6) in part due to the discretization of the beam onto the pixel basis, as shown by the red dotted line in Fig. 3(b). In order to avoid these discretization effects we average over all the possible values of x_0, the distance between the center of the spatial profile of the beam and the pixel basis (see Fig. 3).

The only free parameter in this model is the linear extent of the coherence area a. As a result, it allows us to extract a measure of the "radius" of the coherence area by performing a fit to the data while changing the value of a, as shown in Fig. 2. As can be seen, the behavior of Q_N as a function of transmission obtained from the model provides a very good fit to the measured data. From the model we estimate that the

ratio a/ω_0, where ω_0 is the radius of the conjugate beam at the position of the measurements, is equal to 0.48 for the 1.5 mm Gaussian pump, 0.37 for the 2.3 mm Gaussian pump, 0.27 for the 3.2 mm Gaussian pump, and 0.12 for the 3.0 mm flat-top pump, as indicated in Fig. 2. We have verified that the size of the coherence area obtained with our model for the 1.5 mm pump is consistent with the one estimated in [12] through different techniques for a similar configuration.

As expected, the size of the coherence area is reduced as the size of the pump beam is increased, consistent with the effect on the phase-matching condition of a reduced uncertainty in the k-vector distribution of the pump for larger beam sizes. What is surprising is the reduction in the linear extent of the coherence area by a factor of more than 2 when the Gaussian profile of the pump is changed to a flat-top profile while keeping the size constant. While this large reduction is in part due to the difference in the spread of k-vectors of the different spatial profiles of the pump, it is mainly due to the quadratic dependence of the FWM on the pump field. When the flat-top field profile is squared, its shape is not changed and thus its k-vector distribution stays the same. On the other hand when the Gaussian field profile is squared, its profile gets narrower, which translates into an increase in the spread of k-vectors and thus a larger coherence area.

The reduction in the linear extent of the coherence area obtained with the flat-top pump results in an increase in the number of spatial modes that make up the twin beams by a factor of more than 4. This can be understood by considering that the number of modes that are generated by the process can be estimated by dividing the area of the angular bandwidth of the FWM by the area of the coherence area in the far field [12]. The angular bandwidth is determined by the phase-matching condition, which in turn is mainly determined by the FWM process and is not significantly modified by a change in the pump beam.

IV. EFFECT OF COHERENCE AREA ON RESOLUTION OF ENTANGLED IMAGES

An important aspect of the ability to control the size of the coherence area is the role that it plays in the number of spatial modes that make up the twin beams and thus their information capacity. This dependence can be illustrated by studying the effect of the size of the coherence area on the entangled images that can be generated with the FWM process. In particular, given that the size of the coherence area determines the smallest transverse length scale in the probe and conjugate beams, a change in the size of the coherence will lead to a change in the resolution of the entangled images. To study the effect on the resolution we place a slit pattern in the path of the input probe beam and use an optical system to place its Fourier transform at the center of the cell. After the cell we use a second optical system to perform a second Fourier transform to obtain the image of the slit pattern on the conjugate beam that is generated by the FWM.

We again concentrate on the conjugate beam since all the photons in this beam are generated by the FWM. On the other hand, the probe beam contains a contribution from both the photons generated by the FWM and the input probe photons that do not participate in the FWM. In particular, any of the input k-vectors for the probe that are outside the angular bandwidth of the process will not be amplified. The interaction with the atomic system leads to a different focal plane for the components that participate in the FWM and the ones that do not, leading to some background that contaminates the image for the probe beam. In addition, the spatial pattern of the amplified probe beam is altered by the cross-Kerr effect between the pump and the probe. As a result, a cleaner measure of the effect of the coherence area on the resolution can be obtained through measurements on the conjugate.

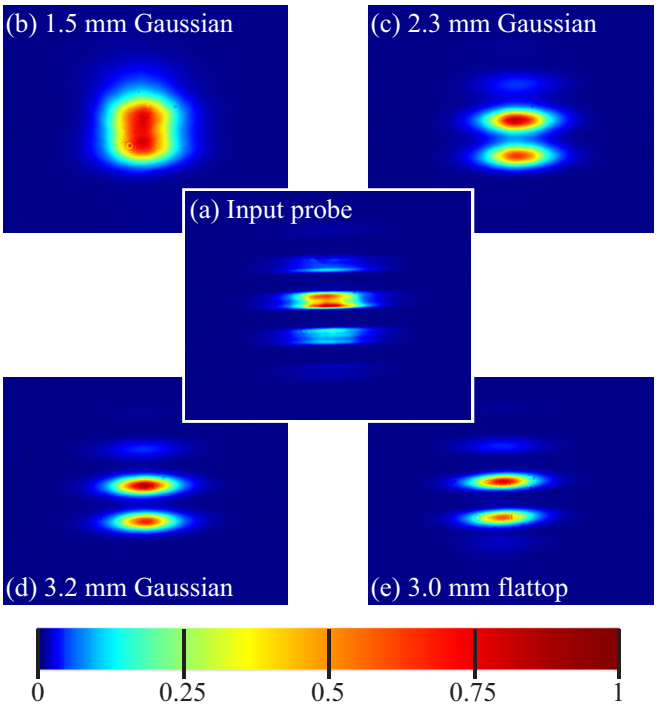

FIG. 4. Effect of size of coherence area on resolution of entangled images. (a) Slit pattern used as an input image for the FWM. Output entangled images for (b) 1.5 mm Gaussian pump beam, (c) 2.3 mm Gaussian pump beam, (d) 3.2 mm Gaussian pump beam, (e) 3.0 mm flat-top pump beam. The images show normalized intensities.

We record the generated image for the four different pumps used to perform the noise measurements. The results are shown in Fig. 4. For the smallest diameter pump beam the fringes cannot be resolved. As we increase the size of the pump the contrast becomes higher and the pattern more closely resembles the input pattern. As can be seen, the best resolution is obtained with the flat-top pump beam, consistent with obtaining the smallest coherence area. This shows that an enhancement in resolution results from a reduction in the size of the coherence area.

V. CONCLUSION

Through a study of the noise properties of entangled twin beams after propagation through a variable size slit, we have shown that it is possible to change the size of the coherence area by changing both the size and spatial profile of the pump beam. In order to extract a measure of the coherence area from

these noise measurements we developed a model based on the concept of a localized coherence area.

Our results show that an increase in the size of the pump leads to a reduction in the size of the coherence area. While this result is expected, we found that a change in the spatial profile of the pump from a Gaussian to a flat top led to a reduction in the linear extent of the coherence area by a factor of more than 2. Such a reduction corresponds to an increase in the number of spatial modes that make up the twin beams by a factor of more than 4.

As we have shown, it is possible to control the number of spatial modes that make up the twin beams, which has an impact on the resolution of the generated entangled images and provides a mechanism to control the information capacity of the twin beams.

ACKNOWLEDGMENTS

This work was funded in part by a grant from the W. M. Keck Foundation.

[1] M. I. Kolobov, Rev. Mod. Phys. **71**, 1539 (1999).
[2] M. I. Kolobov, *Quantum Imaging* (Springer, New York, 2007).
[3] M. I. Kolobov and C. Fabre, Phys. Rev. Lett. **85**, 3789 (2000).
[4] E. Brambilla, L. Caspani, O. Jedrkiewicz, L. A. Lugiato, and A. Gatti, Phys. Rev. A **77**, 053807 (2008).
[5] I. V. Sokolov, M. I. Kolobov, A. Gatti, and L. A. Lugiato, Opt. Commun. **193**, 175 (2001).
[6] D. V. Vasilyev, I. V. Sokolov, and E. S. Polzik, Phys. Rev. A **77**, 020302(R) (2008).
[7] H. Bechmann-Pasquinucci and A. Peres, Phys. Rev. Lett. **85**, 3313 (2000).
[8] G. Brida, M. Genovese, and I. Ruo Berchera, Nat. Photonics **4**, 227 (2010).
[9] H. Pu, W. Zhang, and P. Meystre, Rev. Phys. Lett. **91**, 150407 (2003).
[10] A. Perrin, H. Chang, V. Krachmalnicoff, M. Schellekens, D. Boiron, A. Aspect, and C. I. Westbrook, Phys. Rev. Lett. **99**, 150405 (2007).
[11] W. RuGway, S. S. Hodgman, R. G. Dall, M. T. Johnsson, and A. G. Truscott, Phys. Rev. Lett. **107**, 075301 (2011).
[12] V. Boyer, A. M. Marino, and P. D. Lett, Phys. Rev. Lett. **100**, 143601 (2008).
[13] D. N. Klyshko, Sov. Phys. JETP **67**, 1131 (1988).
[14] T. B. Pittman, D. V. Strekalov, D. N. Klyshko, M. H. Rubin, A. V. Sergienko, and Y. H. Shih, Phys. Rev. A **53**, 2804 (1996).
[15] C. H. Monken, P. H. Souto Ribeiro, and S. Pádua, Phys. Rev. A **57**, 3123 (1998).
[16] G. Molina-Terriza, S. Minardi, Y. Deyanova, C. I. Osorio, M. Hendrych, and J. P. Torres, Phys. Rev. A **72**, 065802 (2005).
[17] S. P. Walborn, C. H. Monken, S. Padua, and P. H. Souto Ribeiro, Phys. Rep. **495**, 87 (2010).
[18] M. Hamar, J. Perina, O. Haderka, and V. Michalek, Phys. Rev. A **81**, 043827 (2010).
[19] C. F. McCormick, A. M. Marino, V. Boyer, and P. D. Lett, Phys. Rev. A **78**, 043816 (2008).
[20] V. Boyer, A. M. Marino, R. C. Pooser, and P. D. Lett, Science **321**, 544 (2008).
[21] P. R. Hemmer, D. P. Katz, J. Donoghue, M. Croningolomb, M. S. Shahriar, and P. Kumar, Opt. Lett. **20**, 982 (1995).
[22] M. S. Shahriar and P. R. Hemmer, Opt. Commun. **158**, 273 (1998).
[23] M. D. Lukin, A. B. Matsko, M. Fleischhauer, and M. O. Scully, Phys. Rev. Lett. **82**, 1847 (1999).
[24] M. D. Lukin, P. R. Hemmer, and M. O. Scully, Adv. At. Mol. Opt. Phys. **42**, 347 (2000).
[25] E. Brambilla, A. Gatti, M. Bache, and L. A. Lugiato, Phys. Rev. A **69**, 023802 (2004).
[26] M. Martinelli, N. Treps, S. Ducci, S. Gigan, A. Maitre, and C. Fabre, Phys. Rev. A **67**, 023808 (2003).
[27] J. Roslund, R. M. de Araujo, S. Jiang, C. Fabre, and N. Treps, Nat. Photonics **8**, 109 (2014).
[28] O. Jedrkiewicz, Y.-K Jiang, E. Brambilla, A. Gatti, M. Bache, L. A. Lugiato, and P. Di Trapani, Phys. Rev. Lett. **93**, 243601 (2004).
[29] C. Fabre, J. B. Fouet, and A. Matre, Opt. Lett. **25**, 76 (2000).
[30] A. M. Marino, J. B. Clark, Q. Glorieux, and P. D. Lett, Eur. Phys. J. D **66** 288 (2012).